Gas-phase interstitially modified intermetallics $R(Fe_{11}Ti)Z_{1-delta}$. I. Magnetic properties of the series $R(Fe_{11}Ti)C_{1-delta}$: R=Y, Nd, Sm, Gd, Tb, Dy, Ho, Er, Tm, Lu

Gas-phase interstitially modified intermetallics $R(Fe_{11}Ti)Z_{1-\delta}$: I. Magnetic properties of the series $R(Fe_{11}Ti)C_{1-\delta}$: R = Y, Nd, Sm, Gd, Tb, Dy, Ho, Er, Tm, Lu

D P F Hurley† and J M D Coey

Department of Pure and Applied Physics, Trinity College, Dublin 2, Ireland

Abstract. A series of tetragonal rare-earth–iron intermetallic carbides $R(Fe_{11}Ti)C_{1-\delta}$ of rare-earths from Nd to Lu have been prepared by reaction of intermetallic powders with butane (C_4H_{10}) at temperatures between 480 °C and 520 °C. On average, the unit cell volume increases upon carbonation by 1.8% across the series. Curie temperatures increase by about 160 K. Values of magnetization at room temperature and 4.2 K are reported. All compounds were found to have easy-axis anisotropy at room temperature, with the exception of Sm which is easy plane. Magnetization curves of aligned samples of the solid solution series $(Y_{1-x}Nd_x)(Fe_{11}Ti)C_{1-\delta}$ give an anisotropy field for the $Nd(Fe_{11}Ti)C_{1-\delta}$ compound of 17(2) T at 4.2 K, and 6(1) T at room temperature. Structural effects of interstitial modification of the intermetallic compounds are discussed, as are the possibilities of introducing interstitial atoms other than H, C and N into these types of alloys via gas-phase reactions.

1. Introduction

Rare-earth– (R–) iron intermetallics can be interstitially modified by reaction with nitrogen, or a nitrogen-containing gas, with dramatic consequences for their magnetic properties. The gas-phase interstitial modification (GIM) process was first applied to the R_2Fe_{17} series [1,2], and then to the iron-rich compounds $R(Fe_{11}Ti)$ [3,4]. Nitrogen occupies the large octahedral interstitial sites adjacent to the rare-earth; (9e sites in the Th_2Zn_{17} structure, 6h sites in the Th_2Ni_{17} structure and 2b sites in $ThMn_{12}$ structure).

These interstitials have two important effects on the magnetism. One is to dilate the lattice, augmenting its volume by several per cent (6.4% for $Y_2Fe_{17}N_{3-\delta}$), which more than doubles the magnitude of the Fe–Fe exchange interaction producing a Curie temperature increase of approximately 400 K across the 2:17 series [2]. The other effect is to modify the crystal field experienced by the 4f shell of the rare-earth. The principal contribution to the crystal field experienced by the 4f electrons in metals comes from the 5d and 6p electron density of the rare-earth atom itself, which Coehoorn points out is governed by bonds formed with the nearest neighbours

[5]. Interstitial atoms with large Miedema parameter (n_{WS}) compared to the rare-earths [6], occupying the 9e/6h (c-plane) sites in the 2:17 structure, will deposit a large electron density at the rare-earth (6c/2b,2d) Wigner–Seitz cell boundaries, producing a large negative contribution to the electric field gradient at these sites. An analogous situation occurs for 1:12 compounds where interstitial 2b sites are along the c-axis occupation of these producing a positive contribution to the electric field gradient at the 2a rare-earth sites [8].

Subsequently, the GIM process was found to be effective for making interstitial carbides, using various hydrocarbon gasses, (CH_4, C_2H_2, C_4H_{10}). Again the first experiments were done on 2:17 compounds [7], and then extended to 1:12 compounds [4]. Here we present the first systematic study of carbides of the $R(Fe_{11}Ti)$ series, for rare-earths from Nd to Lu. The magnetic properties of the parent compounds have been described by Hu *et al* [9].

2. Sample preparation and characterization

The $R(Fe_{11}Ti)$ alloys were prepared by arc melting 3N pure rare-earth metals (R = Y, Nd, Sm, Gd, Tb, Dy, Ho, Er, Tm, Lu) with Fe and Ti. Samples were then wrapped in Ta foil and annealed at 875 °C (1100 °C in the case of Nd) for four days in evacuated quartz tubes. All were shown by x-ray diffraction to be single phase, with the tetragonal $ThMn_{12}$ structure [10]. Small quantities ($\simeq$ 20 mg) of finely ground powders (10–40 μm) were then heated in a thermopiezic analyser at 10 °C min^{-1} in 1 bar of butane to establish the onset temperature of carbon absorption [7]. Carbonation was then achieved by heating $R(Fe_{11}Ti)$ powder at the determined temperature (between 480 and 520 °C in all cases) for up to 2 hours, and then pumping the sample space for 2–3 minutes to eliminate any hydrogen before cooling.

Carbon content determined by weighing, corresponded to $\delta < 0.2$ in the formula $R(Fe_{11}Ti)C_{1-\delta}$. The carbon is expected to enter the 2b octahedral sites since these are the only available interstitial sites in the $ThMn_{12}$ structure of sufficient size to accommodate it, and it has been shown that these are the sites occupied by nitrogen atoms in the corresponding $R(Fe_{11}Ti)N_{1-\delta}$ compounds [11].

The carbonation reaction, in common with the nitrogenation reaction of 1:12 compounds, does not cease at a value of one interstitial atom per formula unit. Absorption of carbon continues with the formation of poorly crystallized iron carbide/rare-earth carbide phases (Fe_3C, RC_2 or TiC) and α–Fe, leading to the destruction of the parent $ThMn_{12}$ structure. The interstitial loading of the compounds must therefore be halted after a suitable period of time (typically 2 hours at the conditions specified previously) to achieve a well-crystallized $R(Fe_{11}Ti)C_{1-\delta}$ interstitial phase, (figure 1). Lattice parameters of the pure carbide phase are included in table 1, and cell volumes are plotted in figure 2(b) below. The unit cell is expanded mainly in the basal plane, $\Delta a/a \simeq 0.8\%$, $\Delta c/c \approx 0.2\%$. All the $R(Fe_{11}Ti)$ compounds form a carbide phase, with a volume expansion averaging 1.8% across the series.

3. Results

Curie temperatures were determined from thermal scans in an applied field of 5 mT. Data were collected during slow cooling of the samples from temperatures of about
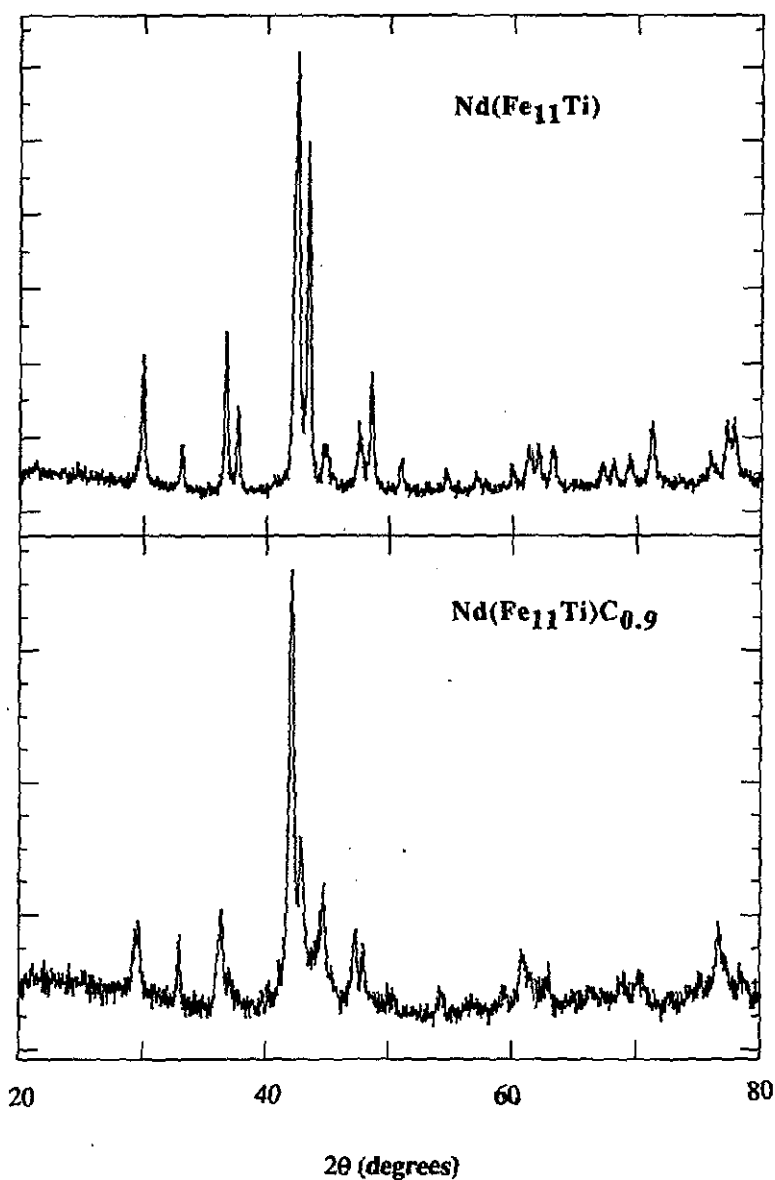
Figure 1. X-ray diffraction patterns of $Nd(Fe_{11}Ti)$ and $Nd(Fe_{11}Ti)C_{1-\delta}$.

800 K and the values of T_c plotted in figure 2 and listed in table 2, refer to the onset of magnetic order in the samples. Values of T_c are about 160 K higher than those for the parent compounds but are $\simeq$ 50 K lower than those of the corresponding nitrides [3,8].

Assuming an effective iron spin $S^* = 1$, molecular field exchange coefficients n_{Fe-Fe} and n_{R-Fe} can be deduced from the Curie temperatures of the heavy rare-

Table 1. Structural and magnetic properties of the series $Y(Fe_{11}Ti)$ and $Y(Fe_{11}Ti)C_{1-\delta}$.

Compound	a (nm)	c (nm)	V (nm³)	$\Delta V/V$ (%)	T_c (K)	$\Delta T_c/T_c$ (%)	$M_s(\mu_B/FU)$		Anisotropy at 290 K
							4.2 K	290 K	
	(1)	(1)	(1)	(3)	(5)	(5)	(4)	(4)	
$Y(Fe_{11}Ti)$	0.851	0.479	0.347	—	524	—	19.1	16.6	axis
$Y(Fe_{11}Ti)C_{1-\delta}$	0.858	0.481	0.354	2.1	678	29.4	20.5	15.5	axis
$Nd(Fe_{11}Ti)$	0.857	0.478	0.351	—	547	—	21.3	16.8	axis
$Nd(Fe_{11}Ti)C_{1-\delta}$	0.862	0.482	0.358	2.0	670	22.5	20.7	20.2	axis
$Sm(Fe_{11}Ti)$	0.855	0.479	0.350	—	584	—	20.1	17.1	axis
$Sm(Fe_{11}Ti)C_{1-\delta}$	0.858	0.480	0.353	0.9	698	19.5	18.0	13.0	plane
$Gd(Fe_{11}Ti)$	0.854	0.480	0.350	—	607	—	12.5	12.5	axis
$Gd(Fe_{11}Ti)C_{1-\delta}$	0.858	0.481	0.354	1.2	734	20.9	14.9	13.2	axis
$Tb(Fe_{11}Ti)$	0.851	0.479	0.347	—	552	—	9.7	10.6	axis
$Tb(Fe_{11}Ti)C_{1-\delta}$	0.857	0.481	0.353	1.7	714	29.3	11.6	12.1	axis
$Dy(Fe_{11}Ti)$	0.849	0.478	0.344	—	534	—	9.7	11.3	axis
$Dy(Fe_{11}Ti)C_{1-\delta}$	0.857	0.479	0.352	2.3	697	30.5	9.6	10.1	axis
$Ho(Fe_{11}Ti)$	0.849	0.479	0.345	—	520	—	9.6	10.2	axis
$Ho(Fe_{11}Ti)C_{1-\delta}$	0.855	0.479	0.350	1.4	691	32.9	8.4	9.4	axis
$Er(Fe_{11}Ti)$	0.848	0.479	0.344	—	505	—	9.2	12.4	axis
$Er(Fe_{11}Ti)C_{1-\delta}$	0.856	0.479	0.351	2.0	685	35.6	11.1	13.1	axis
$Tm(Fe_{11}Ti)$	0.847	0.478	0.343	—	496	—			axis
$Tm(Fe_{11}Ti)C_{1-\delta}$	0.855	0.478	0.349	1.7	686	38.3	16.1	18.9	axis
$Lu(Fe_{11}Ti)$	0.846	0.478	0.342	—	488	—	17.4	15.7	axis
$Lu(Fe_{11}Ti)C_{1-\delta}$	0.855	0.478	0.349	2.0	682	39.7	17.1	16.0	axis

earths using the expressions [12],

$$T_c = \tfrac{1}{2}\left[T_{Fe} + \left(T_{Fe}^2 + 4T_{RFe}^2\right)^{1/2}\right]$$

$$T_{Fe} = n_{Fe-Fe} N_{Fe}\left[4S^*\left(S^* + 1\right)\mu_B^2/3k\right]$$

$$T_{RFe} = n_{R-Fe}|\gamma|\left(N_{Fe} N_R\right)^{1/2}\left\{2g\left[S^*(S^* + 1)J(J + 1)\right]^{1/2}\mu_B^2/3k\right\}.$$

N_{Fe} and N_R are the number of atoms per unit volume, $\gamma = 2(g - 1)/g$, where g is the Landé g factor and J is the rare-earth angular momentum quantum number.

Average values of these coefficients, $\langle n_{Fe-Fe}\rangle$ and $\langle n_{R-Fe}\rangle$ for the series were deduced from T_c data on compounds from Tb to Tm, where the effect of decreasing 4f–5d overlap due to the lanthanide contraction is small [13]. Values obtained are $\langle n_{Fe-Fe}\rangle = 334\ \mu_0$ and $\langle n_{R-Fe}\rangle = 200\ \mu_0$ in the parent compounds and 471 μ_0 and 144 μ_0 in the carbides. The increase of $\simeq 40\%$ in $\langle n_{Fe-Fe}\rangle$ on carbonation results from the enhancement of the Fe–Fe exchange interaction due to the expanded unit cell volume [4, 14, 15]. The reduction in the value of $\langle n_{R-Fe}\rangle$ in the carbided compounds may be due to valence electrons of the rare-earth compound forming covalent bonds with carbon 2p electrons thereby reducing the rare-earth (5d)–iron (3d) wave function overlap.

Magnetization measurements were made using a vibrating sample magnetometer with applied fields up to 6 T at 4.2 K, and up to 1.5 T at room temperature.
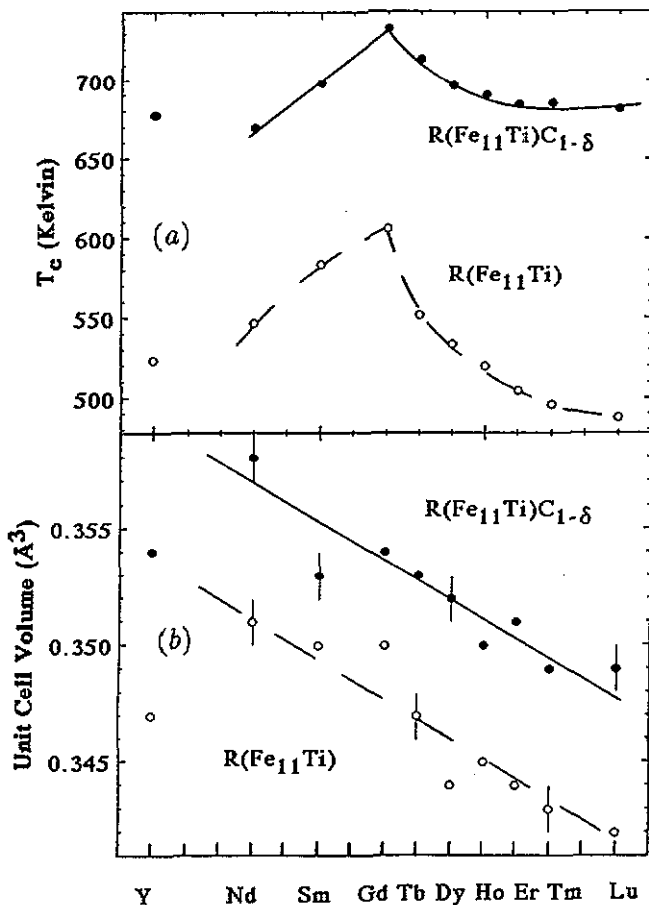
Figure 2. (*a*) Curie temperatures and (*b*) unit cell volumes for the series of rare-earth–iron intermetallics $R(Fe_{11}Ti)$ and $R(Fe_{11}Ti)C_{1-\delta}$.

Each sample consisted of $\simeq 60$ mg of polycrystalline powder in a spherical shape. Values of saturation magnetization were evaluated by extrapolating magnetization as $1/B^2$ tends to zero, after taking account of demagnetizing effects. Free powder magnetization curves for R = Y and Lu give a good estimate of the 3d sublattice magnetization, 20.5(4) μ_B/FU and 17.1(4) μ_B/FU at 4.2 K and 15.5(3) μ_B/FU and 16.0(3) μ_B/FC at 290 K, respectively. Saturation magnetization was greatest for the Nd compound (20.7(4) μ_B/FU at 4.2 K; 20.2(4) μ_B/FU at 290 K) and least for the Ho compound (8.4(2) μ_B/FU at 4.2 K; 9.4(2) μ_B/FU at 290 K). Magnetization values for the series are included in table 1, and plotted in figure 3. These values are consistent with the conventional coupling scheme in rare-earth–iron intermetallics, which yields ferromagnetic order of R and Fe sublattices for the light rare-earths, and ferromagnetic order for the heavy rare-earths.

From x-ray diffraction of aligned powders all samples were found to have easy-axis anisotropy at room temperature, with the exception of Sm which is easy plane.

Carbonation weakens the uniaxial anisotropy of the iron sublattice. From fitting the magnetization curves (taken at 4.2 K) of randomly dispersed fixed powders

Table 2. Electronegativities (ϕ^*), electronegativity difference with yttrium ($\Delta\phi^*_{YX}$), Miedema parameters (n_{WS}) and molar volumes (V) for Y, Fe, Co and those atoms that form gas-phase molecules with hydrogen having molar volumes less than 10 cm³ mol⁻¹, (X = B, C, N, Si, P). Also listed are the enthalpies of formation of binary alloys (at the equiatomic composition, ΔH_{FeX} ΔH_{YX}) of Fe with one of X, and Y with one of X. ϑ_{ch} is defined in the text.

	X							
	Y	Fe	Co	B	C	N	Si	P
ϕ^* (V)	3.20	4.93	5.10	5.30	6.24	6.86	4.70	5.55
$\Delta\phi^*_{YX}$ (V)	—	1.73	1.90	2.10	3.03	3.66	1.50	2.35
n_{WS} (arbitrary)	1.77	5.55	5.36	5.36	5.55	4.49	3.38	4.49
V (cm³ mol⁻¹)	19.9	7.09	6.70	4.70	3.24	4.10	8.60	8.60
Enthalpy of formation ΔH_{FeX} (kJ mol⁻¹);				−38.0	+5.0	+9.0	−26.0	−70.0
Enthalpy of formation ΔH_{YX} (kJ mol⁻¹);				−65.0	−72.0	−180.0	−78.0	−172.0
Chemical, interstitial figure of merit[a]; ϑ_{ch}				0.41	1.07	1.05	0.66	0.59

[a] $\vartheta_{ch} = (\Delta H_{YX} - \Delta H_{FeX})/\Delta H_{YX}$.

[16], values of anisotropy field of 2.3(3) T for $Y(Fe_{11}Ti)C_{1-\delta}$ and 3.4(4) T for the parent $Y(Fe_{11}Ti)$ compound were obtained. To determine the anisotropy field of $Nd(Fe_{11}Ti)C_{1-\delta}$, magnetization of aligned samples was measured parallel and perpendicular to the alignment direction in fields up to 6 T at 4.2 K for the solid solution series $(Y_{1-x}Nd_x)(Fe_{11}Ti)C_{1-\delta}$; ($x$ = 0, 0.4, 0.6, 0.8). B_a was estimated by linear extrapolation of these curves. This was done because we expected that our maximum applied field would be at best only half the value of the anisotropy field of the compound at 4.2 K. We could therefore obtain a more reliable value by extrapolating the anisotropy fields of the series of compounds from the yttrium-rich end where we can more accurately measure B_a, ($B_a/B \approx 1$) to the neodymium-rich side, ($B_a/B \gg 1$) (figure 4). The anisotropy field of the pure $Nd(Fe_{11}Ti)C_{1-\delta}$ compound is thereby found to be 17(2) T at 4.2 K and 6(1) at room temperature.

4. Discussion

4.1. Gas-phase carbonation

Heating the intermetallic compound in butane (C_4H_{10}) leads to the diffusion of both carbon and hydrogen into the $ThMn_{12}$ structure. The rate constant for absorption or desorption is approximately given by $K = \pi^2 D/R^2$, where R is the particle size of the powder and D is the diffusion constant [17]. The R(Fe$_{11}$Ti) powder particle size was in the range 10–40 μm. Diffusion coefficients of hydrogen in rare-earth intermetallics are typically of the order 10^{-9} m²s⁻¹ at temperatures of 500 °C (H in LaNi$_5$; D (800 K) = 4.0 × 10^{-9} m²s⁻¹ [17]). Hence K is $\simeq$ 25 s⁻¹ and we expect total removal of the hydrogen from the intermetallic alloy by our two minute thermal treatment at 500 °C while pumping the sample space, before lowering the temperature of the sample. Carbon is not removed to any significant extent because its diffusion constant is many orders of magnitude smaller ($\simeq 10^{-15}$ m²s⁻¹ at 800 K).

Lattice parameters were refined by getting profiles from the x-ray diffraction patterns using pseudo-Voigt functions of the form $\Omega(2\theta) = \eta L(2\theta, \Gamma_L) + (1 -$
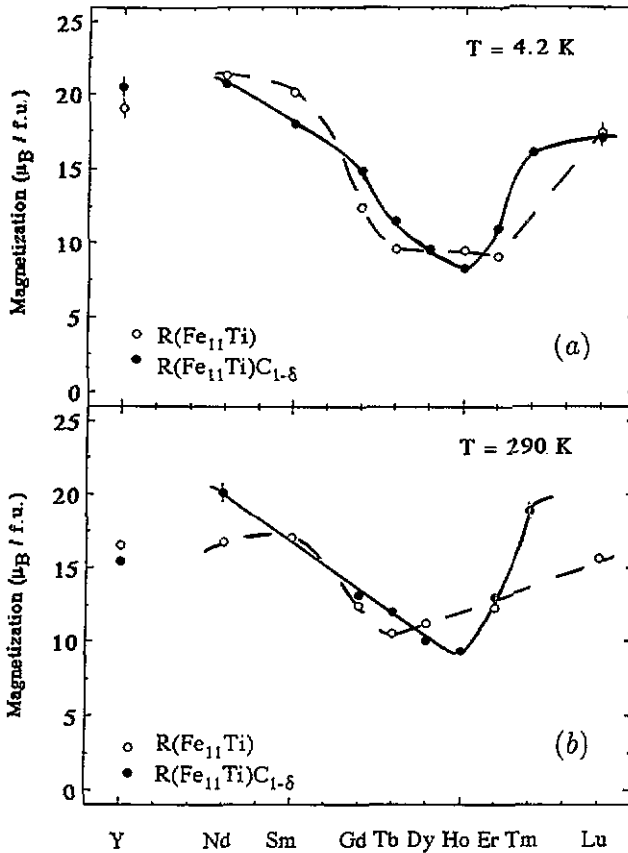
Figure 3. Saturation magnetization for the series of rare-earth–iron intermetallics $R(Fe_{11}Ti)$ and $R(Fe_{11}Ti)C_{1-\delta}$ at (a) 4.2 K and (b) 290 K.

$\eta)G(2\theta, \Gamma_G)$ where L and G denote the Lorentzian and Gaussian components and Γ_L and Γ_G their respective full-widths at half maximum (FWHM). The mixing parameter η which defines the shape of the peak between the limiting Gaussian ($\eta = 0$) and Lorentzian ($\eta = 1$) forms was included as a variable in the refinement. Upon carbonation the diffraction peak profiles were considerably broadened, the FWHM approximately doubling (figure 5), and no satisfactory fit to the data could be obtained by assuming a homogeneous carbide phase of intermediate carbon content. In view of the direct observation of diffusion profiles by Kerr microscopy in $Sm_2Fe_{17}N_{3-\delta}$ by Mukai and Fujimoto [18], and the calculated profiles of Skomski and Coey [19] it is likely that carbon has not diffused all the way to the centre of the larger particles and hence these particles consist of a carbided outer shell with stoichiometry close to $R(Fe_{11}Ti)C$, and a partially carbided or uncarbided inner core. Figure 6(a) shows the distribution profiles expected for spherical particles with $\delta = 0.2, 0.5$ and 0.8 [19].

It can however be clearly seen from figure 5, that the lattice parameters of this core region do not correspond to the lattice parameters of the $R(Fe_{11}Ti)$ bulk material, but are larger. The GIM process in its initial stages produces a pseudo-epitaxial layer of $R(Fe_{11}Ti)Z_{1-\delta}$ grown on $R(Fe_{11}Ti)$ in a spherical geometry. The
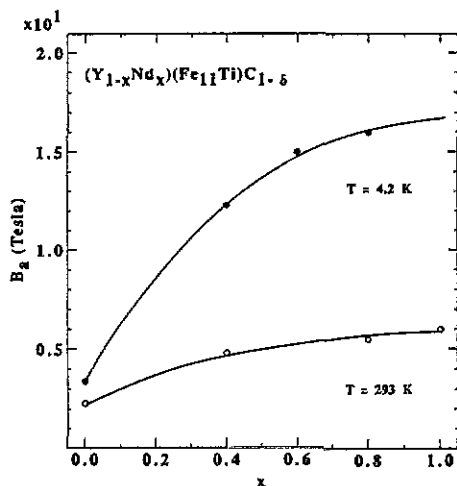
Figure 4. Anisotropy fields as a function of Nd content for the series of compounds $(Y_{1-x}Nd_x)(Fe_{11}Ti)C_{1-\delta}$, values are obtained by linear extrapolation of magnetization curves of aligned samples from a field of 6 T at 4.2 K, and 1.5 T at 293 K.

two phases have an average lattice mismatch of 0.6%. This mismatch is taken up in the strain of both materials. For incomplete interstitial loading of the particles this will produce a strained layer between the two regions, (which may be comparable to the overall dimensions of the particles).

Within this layer, the mismatch strain will cause the $R(Fe_{11}Ti)Z_{1-\delta}$ to be in a state of compression and the $R(Fe_{11}Ti)$ to be in a state of tension. The relative magnitude of these two effects will depend on the radial profile of the interstitial atom content in the grains of the material [19]. This effect is illustrated for various bulk nitrogen contents for the material $Sm(Fe_{11}Ti)N_{1-\delta}$ in figure 6(*b*). The nitride is chosen for this example because it is easier with thermopiezic analysis equipment to accurately measure the bulk nitrogen content from the N_2 gas pressure drop in the sample space [2] than it is to estimate the bulk carbon content from weight gain after treatment in butane; also the expansion is larger than in the corresponding carbide, and the effect is more clearly seen.

4.2. Magnetocrystalline anisotropy

The magnetocrystalline anisotropy in rare-earth transition metal intermetallics is the result of contributions from the 3d and 4f sublattices. The starting $R(Fe_{11}Ti)$ alloys are weak ferromagnets with strong c-axis iron anisotropy. A_{20} is small and negative [20] ($-32\ Ka_0^{-2}$ for the Dy compound and $-143\ Ka_0^{-2}$ for the Sm compound) so there is a further contribution to the easy-axis anisotropy from those rare earths (Sm, Er, Tm) with a positive Stephens coefficient α_J. In fact, all except the Tb compound exhibit uniaxial rare-earth anisotropy at room temperature [9] due to the preponderant contribution of the iron sublattice.

Carbon occupation of the 2b interstitial sites produces an effect analogous to nitrogen; there is a large positive contribution to the electric field gradient at the rare-earth site which changes the sign of A_{20} to positive [3,4]. The tendency for easy-axis anisotropy for all the rare-earths with a negative Stephens coefficient α_J (Nd, Tb, Dy,
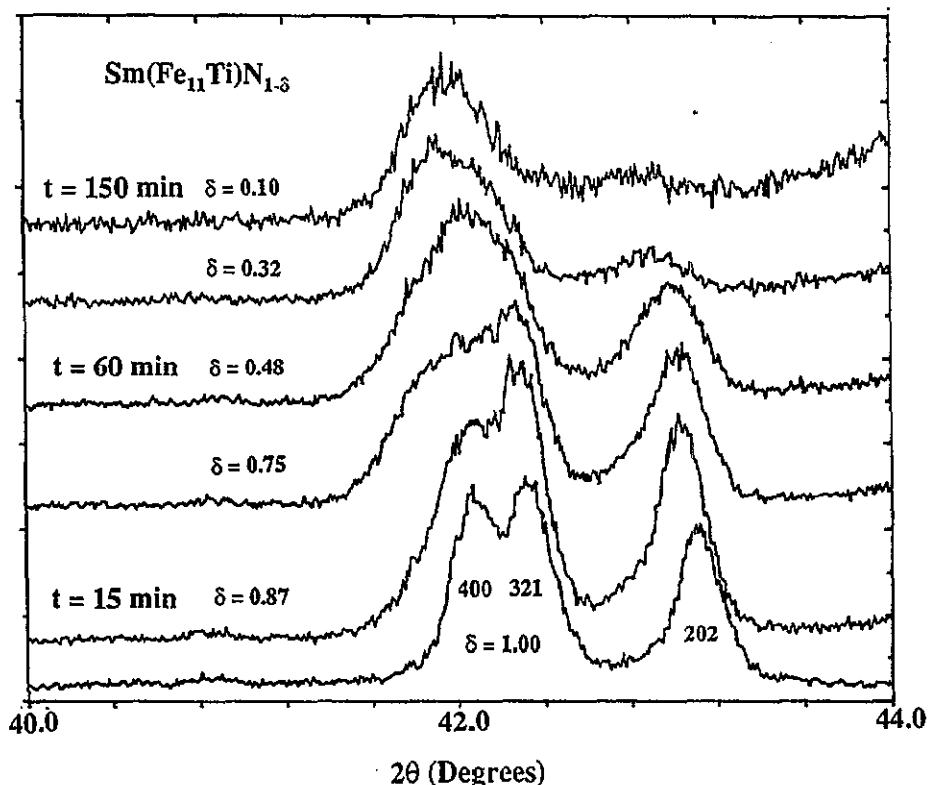
Figure 5. X-ray diffraction showing the 044, 321 and 202 reflections of $Sm(Fe_{11}Ti)N_{1-\delta}$ as a function of bulk nitrogen content. The sample was in treated in N_2 gas for periods of up to 150 minutes at a temperature of 480 °C.

Ho) is enhanced. The anisotropy field of the $Nd(Fe_{11}Ti)C_{1-\delta}$ compound measured at room temperature is $\simeq 6$ T, comparable to that reported for the corresponding nitride (8 T) [3]. The 6 T is made up of a contribution of 2 T from the iron sublattices, and 4 T from the neodymium sublattice (figure 4). From the latter, a value of $A_{20} = 185$ Ka_0^{-2} is deduced for the carbide [21]. Only the Sm compound becomes easy-plane at room temperature (table 1). It is likely that the Er or Tm compounds will exhibit spin reorientations as a function of temperature or carbon content when the easy-axis anisotropy of the iron sublattices is outweighed by the opposing rare-earth contribution. A spin reorientation at 45 K has been reported for $Er(Fe_{11}Ti)N_{1-\delta}$ [3, 22].

4.3. Other interstitials

Finally, we consider the question of whether atoms other than N, C and H can be introduced onto interstitial sites in rare-earth intermetallic compounds by means of the GIM process. Table 2 lists the (metallic state) electronegatives, Miedema parameters, molar volumes and enthalpies of formation of binary alloys at the equiatomic composition, for all those atoms that form gas-phase molecules with hydrogen and that have molar volumes less than 10 cm^3 mol^{-1}. The only atoms which satisfy these criterion
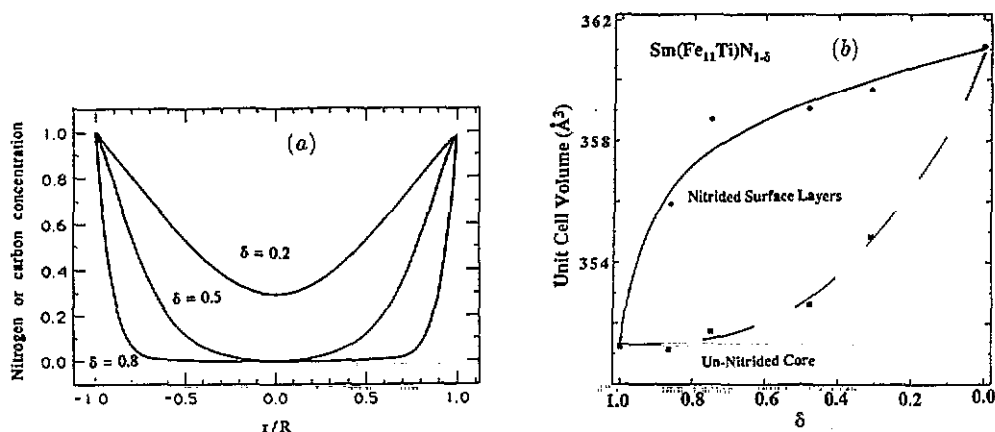
Figure 6. (*a*) Concentration profiles of carbon or nitrogen in a spherical particle with $\delta = 0.2$, 0.5 and 0.8 (after [19]). (*b*) Unit cell volumes of the outer nitrided layer and inner un/partially nitrided core of $Sm(Fe_{11}Ti)N_{1-\delta}$ powders as a function of δ, obtained by profile fitting x-ray diffraction patterns to pseudo-Voigt functions.

that have not been reported as interstitial species are B, Si and P. Possible interstitial transport gases are diborane, silane and phosgene. For both C and N the predicted enthalpy of formation for binary compounds with Fe at a 1:1 composition (ΔH_{FeX}) is small and positive, whereas ΔH_{YX} is large and negative; $\Delta H_{YX} - \Delta H_{FeX}$ being -77 and -189 kJ mol^{-1} respectively for C and N. These atoms therefore have a strong chemical affinity for the rare-earths, and tend to occupy the vacant interstitial sites in the 2:17 and 1:12 structures close to the rare-earth atoms. Also their molar volumes are small 3.24 and 4.10 cm^3 mol^{-1} for C and N respectively, thus they are both structurally and chemically suited as interstitial atoms in this type of intermetallic compound.

Both ΔH_{FeX} and ΔH_{YX} are negative for B, Si and P, $\Delta H_{YX} - \Delta H_{FeX}$ being -27, -52 and -102 kJ mol^{-1} respectively. P and Si unfortunately have larger molar volumes than will allow them to comfortably occupy the interstitial 9e and 2b sites of the 2:17 and 1:12 structures. Boron's volume is only 15% greater than that of nitrogen and should fit on the interstitial sites, but of the five possible interstitials it appears to have the least preference for sites close to the rare-earths. Furthermore boron has a well-known preference for sixfold triangular pyramidic coordination by 3d metals rather than octahedral coordination, as illustrated by the boron site in $Nd_2Fe_{14}B$. To describe the tendency of a specific interstitial species to have a preference to occupy sites close to the rare-earth we define a 'chemical interstitial figure of merit'

$$\vartheta_{ch}(X) = (\Delta H_{YX} - \Delta H_{FeX})/\Delta H_{YX}$$

which parametrizes the difference in enthalpy of formation for the interstitial atom bonding to iron or to a rare-earth, normalized to the energy to form with the rare-earth, which is the preferred case. Values of ϑ_{ch} are given at the bottom of table 2. C and N have the highest values followed in order by Si, P and B. Boron, having a molar volume similar to nitrogen can probably fit onto the interstitial sites in these structures but appears to have little tendency to do so, compared to C and N. It would therefore seem that for chemical (B) and structural (Si, P) reasons these

atoms are less favoured than N or C as possible interstitials for gas-phase interstitial modification.

5. Conclusions

The combination of high Curie temperature, large anisotropy field and the highest saturation magnetization makes $Nd(Fe_{11}Ti)C_{1-\delta}$ the most plausible candidate for development as a hard magnetic material from the present series of compounds. The room-temperature anisotropy field is sufficient to warrant efforts to develop coercivity. Despite the fact that the intrinsic magnetic properties of the $Nd(Fe_{11}Ti)Z_{1-\delta}$; (Z = C, N) compounds are inferior to those of $Sm_2Fe_{17}Z_{3-\delta}$; (Z = C, N) systems, the 1:12 phases might offer a better prospect of producing anisotropic magnet materials, by melt spinning for example. This does not appear to be possible in the case of $Sm_2Fe_{17}Z_{3-\delta}$, as there exist secondary phases such as the metastable $SmFe_7$ [23].

It should be possible to enhance the saturation magnetization of the basic $Nd(Fe_{11}Ti)Z_{1-\delta}$ phase by up to 5% by the partial substitution of some of the Fe by Co in the $ThMn_{12}$ structure [24], as the parent $Nd(Fe_{11}Ti)$ alloy is a weak ferro-magnet [20]. The anisotropy field can also be increased by the partial substitution of Nd by heavy rare-earths such as Tb or Dy, but at the expense of the saturation magnetization. Moreover, the maximum theoretical energy product of the $Nd(Fe_{11}Ti)Z_{1-\delta}$; (Z = C, N) materials (375 kJ m^{-3} for the nitride, 344 kJ m^{-3} for the carbide) are unlikely to surpass those of the $Sm_2Fe_{17}Z_{3-\delta}$ (Z = C, N) compounds (472 kJ m^{-3} for the nitride, 418 kJ m^{-3} for the carbide).

Acknowledgments

References

[1] Coey J M D and Sun H 1990 *J. Magn. Magn. Mater.* **87** L251
[2] Sun H, Coey J M D, Otani Y and Hurley D P F 1990 *J. Phys.: Condens. Matter* **2** 6465
[3] Yang Y-C, Zhang X-D, Kong L-S, Pan Q and G S-L 1991 *Appl. Phys. Lett.* **58** 2042
[4] Coey J M D, Otani Y, Sun H and Hurley D P F 1991 *J. Magn. Soc. Japan* **15** 769
[5] Coehoorn R and Buschow K H J 1991 *J. Appl. Phys.* **69** 5590
[6] de Boer F R, Boom R, Mattens W C M, Miedema A R and Niessen A K 1988 *Cohesion in Metals, Transition Metal Alloys* (Amsterdam: North-Holland)
[7] Coey J M D, Sun H, Otani Y and Hurley D P F 1991 *J. Magn. Magn. Mater.* **98** 76
[8] Coey J M D 1991 *Phys. Scr.* T **39** 21
[9] Hu B-P, Li H-S, Gavigan J P and Coey J M D 1989 *J. Phys.: Condens. Matter* **1** 755
[10] de Mooij D B and Buschow H J 1988 *J. Less-Common Met.* **136** 207
[11] Yang Y-C, Zhang X-D, Kong L-S, Pan Q, Yang J-L, Ding Y-F, Zhang B-S, Ye C-T and Jin L 1991 *Solid State Commun.* **78** 317
[12] Coey J M D, Li H-S, Gavigan J P, Cadogan J M and Hu B-P 1989 *Concerted European Action on Magnets* ed I V Mitchell, J M D Coey, D Givord, I R Harris and R Hanitsch (London: Elsevier) p 76

[13] Li H-S, Li Y-P and Coey J M D 1991 *J. Phys.: Condens. Matter* **3** 7277
[14] Li Y-P and Coey J M D 1992 *Solid State Commun.* **81** 447
[15] Qi Q-N, Li Y-P and Coey J M D 1991 *J. Phys.: Condens. Matter* submitted
[16] Li H-S and Hu B-P 1988 *J. Physique Coll.* **49** C8 513
[17] Buschow K H J, Bouten P C P and Miedema A R 1983 *Rep. Prog. Phys.* **45** 9
[18] Mukai T and Fujimoto K 1992 *J. Magn. Magn. Mater.* **103** 165
[19] Skomski R and Coey J M D 1992 *J. Appl. Phys.* at press
[20] Li H-S and Coey J M D 1991 *Handbook of Magnetic Materials* vol 6, ed K H J Buschow (Amsterdam: North-Holland) p 1
[21] Kuz'min M 1992 *Phys. Rev. B* at press
[22] Yang Y-C, Zhang X-D, Ge S-L, Pan Q, Kong L-S, Li H-L, Yang J-L, Zhang B-S, Ding Y-F and Ye C-T 1991 *J. Appl. Phys.* **70** 6001
[23] Katter M, Wecker J and Schultz 1991 *J. Appl. Phys.* **70** 3188
[24] Yang Y-C, Sun H, Zhang Z-Y, Luo T and Gao J-L 1988 *Solid State Commun.* **68** 175